Exogenous Electricity Flowing through Cyanobacterial Photosystem I Drives CO2 Valorization with High Energy Efficiency

Journal:	*Energy & Environmental Science*
Manuscript ID	EE-ART-05-2021-001526.R2
Article Type:	Paper
Date Submitted by the Author:	25-Aug-2021
Complete List of Authors:	Li, Zhaodong; National Renewable Energy Laboratory Wu, Chao ; National Renewable Energy Laboratory, Biosciences Center Gao, Xiang; National Renewable Energy Laboratory Addison, Bennett; National Renewable Energy Laboratory Shinde, Shrameeta; Miami University Wang, Xin; Texas A&M University, Department of Plant Pathology and Microbiology Chen, Xihan; National Renewable Energy Laboratory Yu, Jianping; DOE National Renewable Energy Laboratory, Svedruzic, Drazenka; National Renewable Energy Laboratory, Blackburn, Jeffrey; NREL, Xiong, Wei; National Renewable Energy Laboratory, Biosciences Center

Exogenous Electricity Flowing through Cyanobacterial Photosystem I Drives CO_2 Valorization with High Energy Efficiency

Zhaodong Li[1], Chao Wu[1†], Xiang Gao[1†], Bennett Addison[1], Shrameeta Shinde[2], Xin Wang[2], Xihan Chen[1], Jianping Yu[1], Drazenka Svedruzic[1], Jeffrey Blackburn[1*], Wei Xiong[1*]

[1]National Renewable Energy Laboratory, Golden, CO.

[2]Department of Microbiology, Miami University, Oxford, OH.

* Correspondence to: Wei.Xiong@nrel.gov and Jeffrey.Blackburn@nrel.gov

† Denotes equal contribution.

Abstract

Nature's biocatalytic processes are driven by photosynthesis, whereby photosystems I and II are connected in series for light-stimulated generation of fuel products or electricity. Externally supplying electricity directly to the photosynthetic electron transfer chain (PETC) has numerous potential benefits, although strategies for achieving this goal have remained elusive. Here we report an integrated photo-electrochemical architecture which shuttles electrons directly to PETC in living cyanobacteria. The cathode of this architecture electrochemically interfaces with cyanobacterial cells that have a lack of photosystem II activity and cannot perform photosynthesis independently. Illumination of the cathode channels electrons from an external circuit to intracellular PETC through photosystem I, ultimately fueling cyanobacterial conversion of CO_2 into acetate. We observed acetate formation when supplying both illumination and exogenous electron under intermittent conditions (e.g., in a 30 s supply plus 30 min interval condition of both light and exogenous electron). The energy conversion efficiency for acetate production under programmed intermittent LED illumination (400 – 700 nm) and exogenous electron supply reached ca. 9%, when taking into account the number of photons and electrons *received* by the biotic system, and ca. 3% for total photons and electrons *supplied* to the cyanobacteria. This approach is applicable for generating various CO_2 reduction products by using engineered cyanobacteria, one of which has enabled electrophototrophic production of ethylene, a broadly used hydrocarbon in the chemical industry. The resulting bio-electrochemical hybrid has the potential to produce fuel chemicals with numerous potential advantages over standalone natural and artificial photosynthetic approaches.

38 **Broader context**

39 Natural photosynthesis with solar irradiance is the primary energy conversion process on
40 earth, driving CO_2 fixation and production of organic compounds. However, its efficiency
41 is limited by the light-harvesting competition between photosystems (PSI and PSII) and
42 photorespiration process. To address these, we assemble an "artificial PSII" which can
43 serve as a new electrochemical energy source in living cyanobacteria. This assembly
44 enabled efficient synthesis of carbon compounds from PSII-inhibited cyanobacterial cells
45 that cannot perform natural photosynthesis alone. The single photosystem (PSI) is
46 powered without light absorption competition by the other (PSII); and production of
47 organic compounds can be energized *via* photovoltaic electrons in addition to visible
48 light. This new photosynthesis concept is proposed to elevate the efficiency ceiling of
49 natural photosynthesis for selective production of fuel chemicals.

50

51

Introduction

Oxygenic photosynthesis is the primary energy conversion process on earth, driving CO_2 fixation and production of organic compounds[1-3]. The central photosynthetic process involves coupled photoexcitation of two reaction center photosystems (PS) I and II (Fig. 1a). Excitation of PSI initiates electron transfer to ferredoxin and NADPH that energizes CO_2-fixing pathways such as the Calvin-Benson-Bassham (CBB) cycle[4]. Photoexcitation of PSII results in oxygen evolution and electron transport from water to plastoquinone (PQ), which then regenerates neutral PSI through a series of reactions in the photosynthetic electron transfer chain (PETC)[4].

Substantial research efforts have focused on leveraging biological photosystems (*e.g.* in algae and cyanobacteria) for sustainable production of energy products from sunlight[5 6]. For example, photosynthetic cyanobacteria have been engineered to produce fuel chemicals and polymers from CO_2[7-12]. However, natural photosynthesis cannot use the full terrestrial solar irradiance, since photosynthetically active radiation (PAR) is limited to a subset of visible light (mostly 400-700nm). Additionally, the natural photosynthetic CO_2 fixation efficiency is diminished by the photorespiration process[13]. Artificial photosynthetic solar-to-fuels cycles have been proposed as alternatives to natural photosynthesis[14-16]. These cycles can achieve high intrinsic energy efficiencies, but typically terminate at hydrogen[17]. To produce carbon-based biofuels, substantial efforts have been made in the past decade on reaction system design, enhancing energy and carbon conversion efficiencies for CO and formate production[18-21]. Further C2 products (e.g., ethylene, ethanol, acetate) were also generated with single-pass efficiencies up to 68%.[22-25] Nevertheless, more advances are still desired for upgrading CO_2 into multi-carbon chemical feedstocks *via* attractive energy-saving routes. We hypothesize that the ultimate goal of producing high-order carbon products at high energy efficiency may be achieved by interfacing natural and artificial photosynthesis in a hybrid system where a photosynthetic organism is synergistically energized by exogenous electrons through PETC. In the inverse of this process, photosynthetic fuel cells utilize "photo-electrogenic" microbes to generate electrical currents [24, 26-28]. For example, cyanobacteria output electrons from PETC to external anode and have shown electrogenic regulation on the circadian rhythm[29]. However, to date there is no integrated

electron transfer strategy that generates chemical energy upon external supply of electricity to biological photosystems.

Here we design, assemble, and optimize a self-sustained hybrid photosynthesis system that aims to circumvent limitations in natural photosynthesis and artificial solar fuel approaches. The crux involves electrochemical reactivation of a PETC-modified cyanobacterium with no PSII activity that cannot perform photosynthesis alone. We introduce a device to shuttle high-energy electrons into this cyanobacterium and a strategy for intermittent light and electricity supply. We demonstrated CO_2 conversion to fuel molecules such as acetate, amino acids and ethylene under this condition. Illuminating single photosystem (PSI) without the light absorption competition by the other (PSII) elevates the efficiency ceiling of natural photosynthesis. The external electricity driving this reaction can be further harvested from multiple renewable sources, such as solar or wind, which are not limited by PAR and therefore enable a broader photosynthetic platform. This innovation introduces the concept of electro-synthetic cyanobacteria with the capability to drive carbon metabolism by both light energy and exogenous electricity. We describe this hybrid as an “electrophototrophic” system, a novel biotic-abiotic platform with the potential to valorize CO_2 in high energy conversion efficiency while producing more complex hydrocarbon fuels than artificial photosynthesis.

Results & discussion

A tailored photoelectrochemical system for electrophototrophy

To energize photosynthesis *via* extracellular electron transport, we first blocked the natural photosynthesis pathway in the cyanobacterium where initial electrons are generated from water splitting in PSII (Fig. 1a). This goal was achieved by either inhibiting PSII activity physiologically *via* site-specific inhibitors [30], or by leveraging a genetically generated PSII knockout mutant[31]. A mutant strain of the cyanobacterium *Synechocystis sp.* PCC 6803 (hereto *Synechocystis*), deficient in chlorophyll *a* binding protein (CP47) in PSII, cannot grow photoautotrophically. In the mutant (hereafter ΔPSII), PSII inactivity was shown by altered 77K fluorescence spectrum (Fig. S1b) and significantly decreased chlorophyll *a* level (Fig. S1c).

112 Next, we designed an electrochemical architecture (Fig. 1b) for exogenous
113 electron delivery to cyanobacteria. This architecture allows physical attachment of
114 cyanobacterial cells to carbon felt and the transparent cathodic fluorine-doped tin oxide
115 (FTO) electrode allows us to investigate light-activated photosystem driven by
116 extracellular electricity. FTO glass substrate faced-up porous carbon felt offers an
117 extremely large interfacial area for bacteria loading (as shown in Fig. S2), excellent
118 electron transport properties, as well as short active species diffusion length for efficient
119 electrochemical reactions[32].

120

121 **Light-dependent exogenous electron transfer to PETC**

122 Electrochemical devices for electrogenesis from photoautotrophically grown
123 *Synechocystis* on anode were reported previously[26, 28, 33]. We first reproduced this
124 electrogenesis process in our newly designed system and examined its electrochemical
125 properties by interfacing biocompatible porous carbon felt with wild-type (WT)
126 *Synechocystis* cells (Fig. 1b). WT *Synechocystis* cells displayed a strong electrogenic
127 response to chopped light under anodic potential (0.4 V vs. Ag/AgCl, Fig. 2a left axis, red
128 solid line), suggesting that physical contact between cells and the extracellular electron-
129 transduction surface enables interfacial electron transfer. In contrast, no photocurrent was
130 observed for ΔPSII under the same conditions (Fig. 2a left panel, red dash line),
131 consistent with previous reports that PSII is the primary source for electrogenesis [24, 33].

132 We next analyzed the properties of ΔPSII as an electron acceptor by applying a
133 cathodic potential (-0.7 V vs. Ag/AgCl). Under this condition, an anoxygenic environment
134 was created in the cathode chamber and electrochemical O_2 evolution occurring on the
135 anode was separated from cathode by a Nafion membrane. The current density in tens
136 of μAcm^{-2} magnitude is relatively steady for both WT and PSII mutant cultures. Intriguingly,
137 illumination of ΔPSII under cathodic potential consistently increased cathodic current
138 density (Fig. 2a left panel, black solid line), whereas the WT *Synechocystis* which carries
139 functional PSII did not produce a photoelectrical response under cathodic bias (Fig. 2a
140 left panel, black dash line). However, such WT strain showed the similar wave-like
141 photoelectrical response in the presence of inhibitor (3-3,4-dichlorophenyl)-1,1-

142 dimethylurea (DCMU) (Fig. S4 and S13). A photoelectrical response was also not
143 observed under cathodic bias with heat-treated dead cells on electrodes (Fig. S3),
144 confirming that the photocurrent observed for *living* ΔPSII cells, although small, is not an
145 artifact. The active PETC components downstream of PSII in the ΔPSII mutant can accept
146 electrons from the external circuit in lieu of the deactivated PSII. Since the electrons
147 provided by PSII from water oxidation in wild type cells would have better electron
148 transport kinetics compared to the external electrons supply to the bacteria, the existence
149 of PSII would induce a more negative potential at the entry point (PQ) of the electron
150 transport chain, which obstructs external electron injection to the bacteria. Without redox
151 reactions by PSII, the light-dependent current response in ΔPSII is in line with the photo-
152 reductive activity of PSI, the excitation of which can transfer electrons to the end of PETC,
153 thus allowing continuous electron input from external circuit. In contrast, photoexcited
154 PSII in the WT strain serves as the predominant electron donor, which could saturate the
155 PETC and diminish photoelectrical response significantly when injecting exogenous
156 electrons from cathode.

157 We next use site-specific redox inhibitors to demonstrate that PETC components
158 downstream of PSII (see Fig. 1a) play a central role in electron flow from extracellular
159 circuit to cyanobacteria. Supplementation of the herbicide (3-3,4-dichlorophenyl)-1,1-
160 dimethylurea (DCMU), a specific inhibitor that blocks the binding site of Q_B in the
161 photosystem[34] (Fig. S4) did not diminish the light-dependent electrical response in ΔPSII
162 cells (Fig. 2b), suggesting that exogenous electrons can flow into the PETC *downstream*
163 of Q_B. Either blocking cytochrome b6f activity with 2,5-dibromo-3-methyl-6-
164 isopropylbenzoquinone (DBMIB)[35] or inhibiting ferredoxin and NADP reduction with
165 phenylmercuric acetate (PMA)[36] resulted in a significant decrease in photoelectrical
166 activity, as evinced by negligible changes of photocurrent density under light on and off
167 (Fig. 2b). Interestingly, the photoelectric response after PMA addition did not completely
168 disappear in the first 300s (Fig, 2b blue curve in the left panel). It indicates a time course
169 in which serial PETC components *upstream* of the PMA inhibition site (ferredoxin-NADP
170 oxidoreductase) are reduced sequentially and thus can still trigger photoelectric response
171 until full reduction. These site-specific inhibitions support the mechanism that exogenous
172 electrons flow through cytochrome b6f, PSI and ultimately reach ferredoxin-NADP

173 oxidoreductase in the PETC. The opposing effect of DBMIB and DCMU further implies
174 that PQ is probably the entry point of exogenous electrons as it is the only PETC
175 component between Q_B and cytochrome b6f.

176 To better understand the biological mechanism underlying the electrophototrophic
177 metabolism observed above, we performed quantitative proteomics analysis on
178 Synechocystis cells (ΔPSII). Specifically, a proteomics comparison was made between
179 ΔPSII cells attached to the carbon felt that were harvested from the cathode chamber and
180 the initial ΔPSII culture where no cathodic bias was ever applied. For cyanobacterial cells
181 undergoing electrophototrophic metabolism (bias-exposed), we found global proteomic
182 adaptation, relative to the initially cultured cells. Pathway enzyme allocation (Fig. S5)
183 displayed an increase of energy metabolism in the proteome including photosynthesis
184 and electron transfer. As a trade-off, the section for translational processing was reduced
185 for the electrophototrophic (bias-exposed) cells, indicating a systematic resource
186 reallocation. Interestingly, we found that upregulated proteins (>1.5 fold changes)
187 included those components for assembling pili, cytochrome b6-f complex iron-sulfur
188 cluster, photosystem I reaction center, ferredoxin and ATP synthase (Fig. S6).
189 Upregulation of these gene products indicate their necessity during electrophototrophic
190 process and is consistent with the proposed energetic mechanism. As such, we conclude
191 that these gene products could potentially play important roles in transfer of exogenous
192 electrons to PETC.

193 **Exogenous electrons energize CO_2-to-fuels conversion with high energy efficiency**

194 Motivated by global demand for CO_2 recycling and production of energetic
195 chemicals, we asked whether the exogenous electrons in our hybrid "electrophototrophic"
196 system could energize CO_2 fixation and conversion to hydrocarbon fuels or fuel
197 feedstocks. To answer this question, we incubated ΔPSII cultures and applied electrical
198 potential with amperometric characterization. Light and electrical bias were systematically
199 investigated as two key variables, and we observe photosynthetic CO_2 fixation and
200 carbon product formation *only* when supplying both illumination and exogenous electron
201 (Fig. 3a, 3b and Fig. S7, S8). Importantly, the longevity of carbon product formation is
202 substantially enhanced under conditions of intermittent illumination and exogenous

203 electron supply. Specifically, experiments discussed in Supplementary Section S(II) (Fig.
204 S17, S18) led us to adopt the condition of supplying photons and electrons for 30 seconds,
205 followed by a 30-minute interval of no supply. Shown in Fig. 3a, this "30 s supply + 30
206 min interval" intermittent condition on the cathode (typical white LED for plant growth, 55
207 μmol m^{-2} s^{-1} on FTO glass) led to a 3.5-fold increase in acetate production compared to
208 its initial value with only cathodic bias (-0.7 V vs. Ag/AgCl, intermittent supply, Fig. S17).
209 In the dark, under the same cathodic bias, acetate concentrations in the culture slightly
210 decreased (from ~270 μM initial residual to ~100 μM), presumably due to non-
211 photoexcited PSI which cannot reduce NADP and fuel carbon metabolism. The viability
212 determined by optical density (OD_{730}) measurements indicate a slight increase under
213 intermittent illumination, while the OD_{730} gradually declined ~40% in dark after 8 days
214 (Fig. S7). In terms of exogenous electron supply, no acetate production was detected
215 without negative electrical bias, even for cells that were illuminated constantly under
216 intermittent program (Fig. S8).

217 As shown in Fig. 3b, acetate production by intermittent illuminated ΔPSII was not
218 found within the first 5 days for application of either no bias or -0.5 V vs. Ag/AgCl. In
219 comparison, once more negative bias (-0.7 V vs. Ag/AgCl, intermittent supply, Fig. S10)
220 was applied (day 6-10), acetate production ensued. Fig. S9 displays acetate yield as a
221 function of various potentials (-0.15 to -0.7V) and indicates that potentials more negative
222 than -0.6 V vs. Ag/AgCl can drive acetate production. Consistently, this threshold potential
223 of -0.6 V (vs. Ag/AgCl) is near the standard reducing potential of electrons in photoexcited
224 PSII (Fig. S9). This correlation implies an energy barrier which needs to be overcome for
225 driving exogenous electron flow into downstream of PETC. Fig. 3b demonstrates that
226 acetate concentration increased steadily for 5 days during incubation under -0.7 V,
227 eventually reaching 650μM. Cell counts for ΔPSII, inferred by OD_{730} measurements,
228 decreased unless a certain bias was applied (Fig. S10). These results support our
229 hypothesis that the primary metabolic processes such as metabolite production and cell
230 maintenance can be energized by highly reductive exogenous electrons, flowing through
231 the PETC.

232 To further investigate the metabolic activities that can be driven by this
233 electrophototrophic system, we performed an isotope tracer analysis by adding ^{13}C-

234 sodium bicarbonate into the ΔPSII culture on the cathode. Bicarbonate can be converted
235 to CO_2 by cyanobacterial carbonic anhydrase[37]. This CO_2 can then drive carbon product
236 formation (acetate) and/or be fixed into biomass *via* cell metabolism. We first examined
237 the labeling fraction of acetate excreted into the medium. The GC-MS revealed the
238 production of ^{13}C-acetic acid, indicating that newly fixed carbons end into this C2 product
239 (Fig. 3c). ^{1}H-NMR spectra demonstrate that acetate was labeled in both methyl and
240 carboxyl carbons (Fig. S11) and allow us to evaluate the energy conversion efficiency in
241 the electro-photosynthetic process. Different from the conventional microbial
242 electrosynthesis processes, both exogenous electrons supply from electrochemical
243 system and the photo-electron coupling involved in this electrophototrophic synthesis.
244 The exogenous electrons for CO_2 conversion to acetate can be quantified by defining the
245 exogenous electrons utilization efficiency ($EEUE_{acetate}$). Over half (61.8%) of exogenous
246 electrons were utilized by ΔPSII for selective acetic acid generation. Taking into account
247 the photon and electron flux *received* by the cyanobacterial cells, the overall light and
248 electrons energy conversion efficiency on our electrophototrophic cyanobacteria is
249 approximately 9.3 %. For total photons and electrons *supplied* to the cyanobacteria, the
250 energy conversion efficiency is approximately 2.8 % (see Supplementary Section S(I),
251 Fig. S14-16 and Table S1 for further discussion of this efficiency calculation). Note that
252 this estimation only reflects the fixed carbons in acetate and does not count those fixed
253 into biomass (*vide infra*).

254 We next analyzed the labeling patterns of seven proteinogenic amino acids that
255 are digested from cell biomass and are directly produced from the central carbon
256 metabolism (Fig. 3d). After four days incubation of ΔPSII with ^{13}C-bicarbonate under
257 white-light illumination, the cathodically biased cultures demonstrate partial ^{13}C-labeling
258 in proteinogenic amino acids and display significantly higher fractional labeling (FL,
259 denoting the proportion of labeled carbons) than the negative control cultures without
260 applied bias. Serine, which can be synthesized from 3-phosphoglycerate, the first CO_2-
261 fixation product of the CBB cycle, demonstrated a 3% FL in comparison with 1% in the
262 negative control. This moderate ^{13}C-accumulation is real because we indeed detected
263 significant increase of the m+1 ^{13}C-pattern in the carboxylic group of serine, consistent
264 with the reaction skeleton of Ribulose-1,5-bisphosphate carboxylase/oxygenase

265 (RuBisCO) (Table S2). As another major CO_2 entry point, ^{13}C-bicarbonate can be fixed
266 by amphibolic reactions (*e.g.* phosphoenolpyruvate carboxylase) to generate
267 oxaloacetate which is the precursor of aspartate and threonine. Consistently, biased
268 cultures have much higher FL (7%) in these two amino acids than those in the unbiased
269 cultures (1%).

270 Interestingly, we observed a new CO_2 fixation pathway activated in cyanobacteria
271 *via* the glycine cleavage system. This pathway was found recently in *Synechocystis*[38] but
272 with no detailed *in vivo* characterization. The metabolic activity of this CO_2-fixing pathway
273 can be reflected by the extremely high FL in glycine (> 30%) when incubated ΔPSII with
274 ^{13}C-bicarbonate under constant white-light illumination for four days. Through this
275 pathway, CO_2 will enter the one-carbon (C1) metabolism *via* formate which then forms
276 the methylene group of glycine. The GC-MS fragment of glycine (Gly_85) represents this
277 methylene group, demonstrating high FL (30%) consistently. In line with labeling evidence,
278 the high activity of the glycine pathway is also reflected by proteomic results that show
279 1.8-fold upregulation of glycine cleavage system H protein (gcvH) in bias-exposed cells
280 (Fig. S6). Altogether, our ^{13}C-tracer analysis, as well as extracellular metabolite analysis,
281 support that exogenous electron supply to cyanobacterial PETC may lead to CO_2 fixation
282 and conversion, demonstrating a functional bioenergetics system that fuels endergonic
283 metabolism.

284 **Electrophototrophic production of ethylene**

285 We further evaluated the hybrid electrophototrophic system for its ability to generate
286 value-added biofuel molecules in addition to acetate and amino acids. To this end, we
287 recruited a *Synechocystis* strain JU547 in which the photosynthetic metabolism was
288 remodeled for high-yield ethylene production[8]. This strain is optimized for overexpression
289 of the heterologous ethylene forming enzyme (EFE) and has achieved photoautotrophic
290 production of ethylene[8]. Here, we applied electric bias to JU547 in the gas-tight cathodic
291 chamber and illuminated the culture constantly. To realize electrophototrophic
292 metabolism, DCMU was supplemented into the culture for inactivation of PSII and the
293 headspace was monitored for ethylene. Shown in Fig. 4, ethylene detection indicates that
294 cells were adapted to this new process. Electrophototrophic production of ethylene

295 sustained for days (Fig. 4b, red circles) and associated with the increase in accumulated
296 charges over time (Fig. 4c). The ethylene titer reached 0.365 mmol $L^{-1}OD_{730}^{-1}$ in Day 8,
297 as we estimated, with average exogenous electrons utilization efficiency ($EEUE_{ethylene}$) of
298 74.9% (see Supplementary Section S(I) for efficiency approximation). In comparison, the
299 negative biological controls without either light or electrical input cannot produce ethylene
300 upon DCMU supplementation (blue line and black line, respectively). Another control
301 experiment, in which cyanobacterial cells were not applied, did not produce ethylene (data
302 not shown), excluding the possibility of abiotic ethylene production upon electrochemistry
303 alone. Collectively, these tests displayed the validity and generality of our
304 electrophototrophic approach for tailored production of fuel molecules from cyanobacteria.

305 **Discussion**

306 Electrification of biocatalysis, such as microbial electrosynthesis (MES), seeks
307 efficient conversion of CO_2 to fuels and chemical feedstocks[39-43], representing a strategic
308 direction to meet global energy demand. As a novel MES form, our proof-of-concept
309 electro-photosynthetic system leverages exogenous electrons to supplement
310 photosynthetic energy conversion for driving CO_2 fixation and conversion. Cyanobacterial
311 cells without PSII can sustain their metabolic viability on an electrode surface and produce
312 acetate, the primary excreting product as well as non-native ethylene (Fig. 3 and Fig. 4).

313 Compared with state-of-the-art microbial electrosynthesis systems, which have
314 also realized acetate production from CO_2, our system has merits that could ensure an
315 enabling and practical technology. First, cyanobacteria have been well developed to be
316 a photosynthetic cell factory for more than a decade. They can serve as microbial chasses
317 for production of a variety of energy products with increasing productivities[44, 45]. Second,
318 in contrast to current electrosynthetic microbes, most of which are strict anaerobes,
319 cyanobacteria are much more tolerant to oxygen and can also grow anaerobically either
320 in cathodal chamber or dark regime during day/night cycle. This flexibility offers additional
321 ease in operations when preparing precultures and manipulating bio-electrochemical
322 processes. Third, cyanobacteria can take up gaseous CO_2 as well as soluble inorganic
323 carbons (e.g., bicarbonate). Effective CO_2 concentrating mechanisms (CCM) have been
324 evolved in cyanobacteria to facilitate transport and utilization of inorganic carbon

substrates, offering an exceptional benefit in mass transfer[46]. Last but not least, cyanobacterial metabolism has been tailored for CO_2 fixation, while electrosynthetic microbes (e.g. acetogens) rely on the Wood-Ljungdahl pathway (WLP) for carbon fixation. WLP is one of the oldest biochemical pathways and has to couple CO_2 fixation to energy conservation at the thermodynamic limit of life[47]. Due to the complexity of WLP pathway enzymes, genetic engineering efforts that can improve WLP catalytic efficiency have not been reported. In contrast, cyanobacteria demonstrate evolutionary advantages in metabolism. The Calvin-Benson cycle in cyanobacteria is the most broadly used CO_2-fixation pathway on earth and is much less restricted thermodynamically. Moreover, other carbon-conserving pathways (e.g. phosphoketolase pathway)[8] exist in cyanobacteria, allowing versatile metabolic functions and could enable more efficient electrosynthesis.

Here, growing photosystems-modified cyanobacteria in a photoelectrochemical architecture allows us to expand the means by which photosynthetic organisms produce fuels and chemicals. Such hybrid systems can access new pathways beyond canonical photosynthesis, the inefficiency of which largely arises from the use of two photochemical systems with similar absorption thresholds. The two photosystems (PSII, PSI) compete for the same regions of the solar spectrum, cutting energy efficiency nearly in half compared with what might be achieved if the bandgaps were optimized to use different regions of the spectrum[2, 48]. Additionally, as originally proposed by Blankenship and co-authors[2], new tandem configuration strategies that *e.g.* pair two photosystems activating in the different spectrum ranges, may increase the theoretical upper bound of natural photosynthesis. As a thought experiment, we discuss a potential vision (and associated challenges) of such a hybrid system, based on our electrophototroph, in the supporting information (Fig. S19 and associated discussion, Supplementary Section S(III)).

An additional merit for this hybrid photosynthesis approach arises from the fact that inactivated PSII does not evolve O_2 as the photosynthetic byproduct. Suppressed O_2 evolution (locally in the cyanobacteria, not on the anode where O_2 evolution is still necessary to provide the electrons needed at the cathode) minimizes the propensity for RuBisCO to fix O_2 as a competitive substrate for CO_2. In natural photosynthesis, substrate competition initiates an energy-intensive recovery process of photorespiration[49] that can consume up to 25% of the initially stored energy[50], a substantial source of inefficiency.

Interestingly, although photorespiration also plays a biosynthetic role in metabolic processes, *e.g*. supplying glycine as an essential metabolite[49], this role in hybrid photosynthesis seems to be substitutable with redundant pathways, such as the glycine cleavage system[38]. This notion is strongly supported by the presence of pathway genes in cyanobacterial genome in line with isotope labeling patterns and proteomic data as we provided here. Decrease in photorespiration thus represents an additional opportunity in the hybrid system to raise the theoretical limits of photosynthesis.

More importantly, the hybrid system introduces a unique strategy for managing photosynthetic outcomes. In natural photosynthesis, linear electron flow occurring between two photochemical systems produces ATP and NADPH as energetic currency, and their proportions are regulated for various biosynthetic purposes. Phototrophs containing only PSI implement electron transport whereby electrons can be recycled from either reduced ferredoxin or NADPH to PQ, and subsequently to the cytochrome b6f complex[51]. Such *cyclic flow* generates a pH gradient (and thus ATP), but without the accumulation of reduced species for biosynthesis[52]. However, this study shows that *Synechocystis* carrying single PSI can be electrically energized to fix CO_2 and generate building blocks of biomass, evinced by labeled proteinogenic amino acids from ^{13}C-bicarbonate. This study further indicates that the hybrid photo-electrochemical process demonstrated here could enable on-demand control over the proportion of linear versus cyclic electron flow to tailor the stoichiometric ratios of ATP/NADPH and ultimate photosynthetic products. To achieve this goal, Nature evolved complicated regulatory mechanisms to tune the ratio of PSI to PSII.[53, 54] In the photoelectrochemical hybrid demonstrated here, the ratios of energetic currency and products could instead be regulated through the injection of exogenous electrons, which creates an artificial linear electron flux that can be varied on-demand relative to cyclic electron flow by tuning the cathodic current density and/or incident photon flux. Since this hybrid approach is not tailored by evolution, it will be less constrained by the natural needs/environments to implement. Instead, the hybrid can be optimized in well-designed conditions for targeted ATP/NADPH ratio. Reengineering the system, for example on the biotic-abiotic interface, is expected to improve overall efficiency for tunable electron transfer. Moving forward

386 towards practical systems will also benefit from strategies for *continuous* supply of
387 photons and exogenous electrons to the electrophototrophic hybrid system.

388 Taken together, the hybrid electrophototroph demonstrated here drives exogenous
389 electrochemical energy to replenish the universal energy and redox currency in living
390 cyanobacteria for biosynthesis. Considering its functionality and a number of advantages
391 over pure natural/artificial photosynthesis, we posit that the development of this bio-
392 electrochemical platform has the potential to enable new avenues to couple renewable
393 electricity with photobiological activities, a practical approach for production of
394 hydrocarbon fuels from sun and CO_2.

395

396 **Methods**

397 Characterization of PSII knockout mutant in *Synechocystis*

398 The PSII deficient *Synechocystis* was a gift from Dr. Wim Vermaas at Arizona State
399 University. This mutant was generated by deleting the psbB gene which encodes
400 chlorophyll-binding protein CP-47 in PSII of *Synechocystis*.[31] The *slr0906* open reading
401 frame (ORF) encoding psbB was disrupted by inserting an antibiotic-resistance gene
402 cassette, replacing a part of the coding sequence. The genotype of the mutant was
403 verified by a PCR analysis using primers 0906_VF and 0906_VR (0906-VF:
404 CGTTACTAGAAGGAGCGTCA, 0906-VR: GGTACCTGGGGAGAGTAGAT). The ΔPSII
405 mutant and wild type *Synechocystis* were measured by fluorescence emission spectra
406 (77K) using a 435-nm excitation wavelength. The chlorophyll *a* level in the mutant was
407 quantitated after methanol extraction by measuring the absorbance of the supernatant at
408 663 nm, using glass cuvettes.

409 Cyanobacteria-electrode hybrid system

410 The PSII deficient *Synechocystis* (Δslr0906) was first inoculated and cultured
411 photoheterotrophically in BG11 medium with addition of 5mM glucose, under 30-50 μmol
412 $m^{-2}s^{-1}$ illumination at 30°C. Exponentially growing cells were collected for further
413 applications.

414 In the following procedure, the tailored electrochemical H-cell with three-electrode
415 configuration was applied for the electrochemical process. The reference and counter
416 electrodes were silver/silver chloride electrode and Pt, respectively. The working
417 electrode and reference electrode (CH Instruments, Inc.) were in the bottom chamber and
418 the Pt wire counter electrode was in the top chamber. A Nafion 117 membrane (Sigma-
419 Aldrich) separates the two chambers. Each chamber has an inlet/outlet. The exponentially
420 growing culture was centrifuged 8 min at 4000 rpm, separated from the supernatant and
421 re-dispersed in the medium (BG11+ bicarbonate, pH = 7.8). This process was repeated
422 three times in order to remove the residual glucose. The cell pellet was then dispersed in
423 the medium (BG11+ bicarbonate, pH = 7.8) for the electrophototrophic experiment. A ~7
424 ml culture was transferred to the cathode chamber of the H-cell, where the culture was
425 illuminated from the bottom transparent window. The device was air-tight and maintained
426 at 30 °C for the duration of the electrochemical characterization.

427 Photoelectrochemical characterization

428 During the electrochemical incubation, a typical amperometry (i-t) procedure (CH
429 Instruments, Inc.) was conducted to check the ability of ΔPSII cyanobacteria as an
430 electron acceptor under illumination. The illumination used in the experiment is the typical
431 white LED illumination for cyanobacteria growth (Photon Systems Instrument, Czech
432 Republic). Photon flux was measured by Li-250A Light Meter with a quantum sensor (LI-
433 COR Biosciences, NE, USA). It was conducted at different potentials (*vs.* Ag/AgCl,
434 saturated KCl solution). Typically, the chopped light (60s on/off) was used for the
435 photocurrent response measurement in photoelectrochemical process. The programmed
436 "30 s supply + 30 min interval" of both illumination and exogenous electron supply were
437 utilized as the conditions for long-term electrophototrophic experiment. A 0.15 ml culture
438 was taken every day for OD_{730} and metabolite analysis.

439 PETC inhibition assay

440 Three PETC inhibitors: 3-(3,4-dichlorophenyl)-1,1-dimethylurea (DCMU), 2,5-
441 dibromomethylisopropyl-1,4-benzoquinone (DBMIB), and phenylmercury acetate (PMA)
442 were obtained from Sigma-Aldrich. They were dissolved in dimethyl sulfoxide for use. The
443 working concentrations of DCMU, DBMIB and PMA were based on previous report[24],

444 which were 20 μM, 50 μM, 200 μM, respectively. The photoelectrochemical
445 measurements were conducted after the inhibitors were supplemented into the culture for
446 10 min.

447 Proteome measurement and analysis

448 Proteome of electrophototrophic Synechocystis ΔPSII mutants 48 hours after a
449 shift from non-EC (no electricity applied) to EC (electricity applied) condition was analyzed.
450 The growth condition of ΔPSII mutant followed the same procedures as described above.
451 Cells from biofilms on electrode and planktonic cells were separately harvested and
452 analyzed. The proteomic analysis of ΔPSII mutant were conducted following the same
453 method in our previous report[55]. 10 μg of trypsin digested peptides from each sample
454 were loaded onto a C18 capillary column coupled to a Thermo LTQ Orbitrap mass
455 spectrometry (Thermo-Scientific, Rockford, IL). The peptide identity was analyzed at the
456 resolution of 30,000. Dynamic exclusion was enabled in this case with the setup of repeat
457 count of 1, repeat duration of 30 seconds, and exclusion duration of 90 seconds. The
458 peptide identify was obtained by searching the tandem MS spectra using Patternlab for
459 Proteomics[56].

460 Electron microscopy characterization

461 After the electrochemistry process, the carbon felt electrode was fixed in 2.5%
462 glutaraldehyde in phosphate buffer under 4 °C for 2 h. The samples then underwent a
463 MilliQ water postfix wash and dehydration (~ 24 h in a high vacuum desiccator). Scanning
464 Electron Microscopy (Hitachi S-4800 SEM) was applied to characterize the surface
465 morphology. Samples were imaged at 3 kV acceleration, 7–10 mm working distance.

466 Quantitative analysis of acetate

467 We measured the excretion of acetate from *Synechocystis* using the following
468 method. The culture samples were collected and the supernatant was separated from
469 cells by filtration through 0.2 μM-diameter nylon membrane (Acrodisc®). Acetate
470 concentration in each culture was analyzed with High Performance Liquid
471 Chromatography (HPLC, Agilent Technologies1200 series) by injecting 25 μL samples
472 into an HPLC column (Bio-Rad Aminex HPX-87H), eluting with 5mM sulfuric acid at a
473 flow rate of 0.6 ml/min, and detecting by a refractive index detector (retention time for

474 acetate: 15.2 min). Standard samples with five different acetate concentrations (2.5, 5,
475 10, 25, and 50 mM) were used for quantification (R^2 = 0.99839).

476 ^{13}C- isotope tracer analysis to track carbon fixation

477 ^{13}C-bicarbonate was supplied during the electrochemical procedures to monitor
478 carbon metabolism in the photoelectrochemical environment. The ^{13}C-labeled fraction of
479 acetate and protein-bound amino acids were measured by NMR and gas
480 chromatography-mass spectrometry (GC-MS), respectively. Exponentially growing ΔPSII
481 cells were suspended in BG-11 medium supplemented with 100mM ^{13}C-labeled sodium
482 bicarbonate. The culture was applied in the electrochemical device under sunlight
483 simulated illumination (white LED, 55 μmol m^{-2} s^{-1}on FTO glass). Cultures were sampled
484 at 0 hour, 2 day, 4 day and 5 day.

485 The sample treatment and GC-MS analysis were performed as previous
486 reported.[57] Briefly, 5mL of sampled cultures were centrifuged at 10,000 g for 1 minute,
487 the cell pellets were digested in 500μL 6M HCl at 105°C for 12 hours. The hydrolysate
488 was dried under nitrogen gas flow at 65°C, dissolved in 50 μL water-free
489 dimethylformamide. For the GC-MS measurement the proteinogenic amino acids were
490 derivatized prior to analysis. The dried hydrolysate, dissolved in pyridine was derivatized
491 by N-tert-butyldimethylsilyl-N-methyltrifluoroacetamide (TBDMS) with 1% tert-butyl-
492 dimethylchlorosilane at 85°C for 60 min. 1 μL of the sample in the organic phase was
493 loaded on the Agilent GC-6890 gas chromatography equipped with a Agilent 19091J-413
494 column (30m×0.32mm×0.25μm) directly connected to a MS-5975C mass spectrometer.
495 Helium was used as the carrier gas. The oven temperature was initially held at 50°C for
496 2 min; then raised to 150°C at 5°C /min and held at that value for 2 min; finally, it was
497 raised to 320°C at 7°C /min, and held at that final value for 2 min. Other settings included
498 splitless and electron impact ionization (EI) at 70 eV. The FLs of alanine, aspartate,
499 glutamate, glycine, phenylalanine, serine, threonine was analyzed.

500 To analyze the isotope labeling pattern of amino acids, a mass isotopomer
501 distribution vector, MDV_{α}, was assigned according to Nanchen *et al* [58].

$$MDV_{\alpha} = \begin{bmatrix} (m_0) \\ (m_1) \\ \vdots \\ (m_n) \end{bmatrix} \quad \sum_{i=0}^{n} m_i = 1 \qquad (1)$$

where m_0 is the fractional abundance of molecules with mono-isotopic mass and $m_{i>0}$ is the abundance of fragments with heavier masses. The GC-MS data were corrected for the naturally occurring isotopes of oxygen (O), hydrogen (H) and carbon (C) atoms using a correction matrix (Eq. 2) as described by Nanchen *et al* [58].

$$MDV_{\alpha}^{*} = C_{corr,COH}^{-1} . MDV_{\alpha} \qquad (2)$$

where MDV_{α}^{*} is the corrected mass isotopomer distribution vector and $C_{corr,COH}^{-1}$ is the correction matrix. According to Equation 3, the resulting MDV_{α}^{*} values were then used to assess the fractional labeling (FL) of amino acids whose carbon skeletons are derived from their precursors in the central carbon metabolism.

$$FL = \frac{\sum_{i=0}^{n} i.mi}{n.\sum_{i=0}^{n} mi} \qquad (3)$$

where *n* represents the number of carbon atoms in the amino acid and *i* is the mass isotopomer. Corrected MDV for seven proteinogenic amino acids is shown in Table S1.

NMR samples were prepared by spiking neat solution with 50 microliters of D_2O with a 10x concentrated solution of Phosphate buffer and TMSP (Sodium-3-Trimethylsilylpropinoate-d4, Cambridge Isotopes), for a final solution of 550 microliters, 70 mM Phosphate buffer and 0.91 mM TMSP as an internal chemical shift and concentration standard. All ^{1}H NMR experiments were collected on a 600 MHz Bruker Avance III NMR spectrometer equipped with a Bruker 5 mm 1H/X broadband probe with sample temperature controlled at 25°C. Acquisition parameters were as follows: the 1D NOESY-presaturation experiment was used (Bruker pulse program noesypr1d) with a water presaturation pulse equivalent to 12 Hz field strength during both a 5 second relaxation delay and during a 50 millisecond NOESY mixing time. Data was collected with a 20 ppm spectral window, 256 scans with 8 dummy scans, and 128k acquired points

equivalent to 5.5 seconds of acquisition time. All spectra were processed using MestreNova version 14, which included 0.2 Hz exponential line-broadening before Fourier transform, manual phase correction, polynomial baseline correction, and chemical shift referencing to TMSP at 0.0 ppm. To obtain quantifications and isotopomer ratios, ^{1}H spectral deconvolution was performed using the MestreNova Line Fitting tool. Peak areas were exported to Microsoft Excel for further analysis.

Experimental analysis for electrophototrophic ethylene production

An engineered ethylene-producing strain Synechocystis JU547 was used. Its ability in ethylene production was verified under regular phototrophic condition[8]. In terms of the electrophototrophic incubation, a typical amperometry (i-t) procedure (CH Instruments, Inc.) was conducted to check the ability of this strain as an electron acceptor under illumination and PSII inactivation. The PSII of the JU547 cells was inhibited by supplementing 20 μM DCMU. Exogenous electron supply was conducted at -0.7 V (*vs.* Ag/AgCl, saturated KCl solution). The culture was applied in the electrochemical device under illumination (white LED, 55 μmol m^{-2} s^{-1}). To set up negative controls, we applied the same condition for Synechocystis JU547 cultures as well as electrochemical devices only except applying either illumination or light. All setups were gas tight. For ethylene quantification, a 200μL gas sample was taken from the head space and injected into GC as our previous report described[59].

References

1. M. F. Hohmann-Marriott and R. E. Blankenship, *Annual Review of Plant Biology*, 2011, **62**, 515-548.
2. R. E. Blankenship, D. M. Tiede, J. Barber, G. W. Brudvig, G. Fleming, M. Ghirardi, M. R. Gunner, W. Junge, D. M. Kramer, A. Melis, T. A. Moore, C. C. Moser, D. G. Nocera, A. J. Nozik, D. R. Ort, W. W. Parson, R. C. Prince and R. T. Sayre, *Science*, 2011, **332**, 805-809.
3. M. Hambourger, G. F. Moore, D. M. Kramer, D. Gust, A. L. Moore and T. A. Moore, *Chem Soc Rev*, 2009, **38**, 25-35.
4. J. H. A. Nugent, *European Journal of Biochemistry*, 1996, **237**, 519-531.
5. D. R. Georgianna and S. P. Mayfield, *Nature*, 2012, **488**, 329.
6. M. Rosenbaum, Z. He and L. T. Angenent, *Current Opinion in Biotechnology*, 2010, **21**, 259-264.

7. N. E. Nozzi, J. W. K. Oliver and S. Atsumi, *Frontiers in bioengineering and biotechnology*, 2013, **1**, 7-7.
8. W. Xiong, J. A. Morgan, J. Ungerer, B. Wang, P.-C. Maness and J. Yu, *Nature Plants*, 2015, **1**, 15053.
9. E. I. Lan and J. C. Liao, *Proceedings of the National Academy of Sciences*, 2012, **109**, 6018-6023.
10. T. Kusakabe, T. Tatsuke, K. Tsuruno, Y. Hirokawa, S. Atsumi, J. C. Liao and T. Hanai, *Metabolic Engineering*, 2013, **20**, 101-108.
11. A. Schirmer, M. A. Rude, X. Li, E. Popova and S. B. del Cardayre, *Science*, 2010, **329**, 559-562.
12. A. K. Singh and N. Mallick, *FEMS Microbiology Letters*, 2017, **364**.
13. P. Pospíšil, *Biochimica et Biophysica Acta (BBA) - Bioenergetics*, 2009, **1787**, 1151-1160.
14. D. K. Dogutan and D. G. Nocera, *Accounts of Chemical Research*, 2019, **52**, 3143-3148.
15. D. G. Nocera, *Accounts of Chemical Research*, 2012, **45**, 767-776.
16. N. S. Lewis, *Science*, 2016, **351**, aad1920.
17. T. R. Cook, D. K. Dogutan, S. Y. Reece, Y. Surendranath, T. S. Teets and D. G. Nocera, *Chemical Reviews*, 2010, **110**, 6474-6502.
18. W.-H. Cheng, M. H. Richter, I. Sullivan, D. M. Larson, C. Xiang, B. S. Brunschwig and H. A. Atwater, *ACS Energy Letters*, 2020, **5**, 470-476.
19. S. Verma, Y. Hamasaki, C. Kim, W. Huang, S. Lu, H.-R. M. Jhong, A. A. Gewirth, T. Fujigaya, N. Nakashima and P. J. A. Kenis, *ACS Energy Letters*, 2017, **3**, 193-198.
20. F. P. Garcia de Arquer, C. T. Dinh, A. Ozden, J. Wicks, C. McCallum, A. R. Kirmani, D. H. Nam, C. Gabardo, A. Seifitokaldani, X. Wang, Y. C. Li, F. Li, J. Edwards, L. J. Richter, S. J. Thorpe, D. Sinton and E. H. Sargent, *Science*, 2020, **367**, 661-666.
21. J. Li, Y. Kuang, Y. Meng, X. Tian, W. H. Hung, X. Zhang, A. Li, M. Xu, W. Zhou, C. S. Ku, C. Y. Chiang, G. Zhu, J. Guo, X. Sun and H. Dai, *J Am Chem Soc*, 2020, **142**, 7276-7282.
22. C.-T. Dinh, Y. C. Li and E. H. Sargent, *Joule*, 2019, **3**, 13-15.
23. C. T. Dinh, T. Burdyny, M. G. Kibria, A. Seifitokaldani, C. M. Gabardo, F. P. Garcia de Arquer, A. Kiani, J. P. Edwards, P. De Luna, O. S. Bushuyev, C. Zou, R. Quintero-Bermudez, Y. Pang, D. Sinton and E. H. Sargent, *Science*, 2018, **360**, 783-787.
24. M. Torimura, A. Miki, A. Wadano, K. Kano and T. Ikeda, *Journal of Electroanalytical Chemistry*, 2001, **496**, 21-28.
25. S. Ma, M. Sadakiyo, R. Luo, M. Heima, M. Yamauchi and P. J. A. Kenis, *Journal of Power Sources*, 2016, **301**, 219-228.
26. J. M. Pisciotta, Y. Zou and I. V. Baskakov, *PLoS One*, 2010, **5**, e10821-e10821.
27. K. Tanaka, N. Kashiwagi and T. Ogawa, *Journal of Chemical Technology & Biotechnology*, 1988, **42**, 235-240.
28. M. Sawa, A. Fantuzzi, P. Bombelli, C. J. Howe, K. Hellgardt and P. J. Nixon, *Nat Commun*, 2017, **8**, 1327-1327.

29. Y. Lu, K. Nishio, S. Matsuda, Y. Toshima, H. Ito, T. Konno, K. Ishihara, S. Kato, K. Hashimoto and S. Nakanishi, *Angew Chem Int Ed Engl*, 2014, **53**, 2208-2211.
30. A. Trebst, in *Methods in Enzymology*, ed. A. San Pietro, Academic Press, 1980, vol. 69, pp. 675-715.
31. W. F. J. Vermaas, J. G. K. Williams, A. W. Rutherford, P. Mathis and C. J. Arntzen, *Proceedings of the National Academy of Sciences*, 1986, **83**, 9474-9477.
32. C. Zhu, H. Li, S. Fu, D. Du and Y. Lin, *Chem Soc Rev*, 2016, **45**, 517-531.
33. K. L. Saar, P. Bombelli, D. J. Lea-Smith, T. Call, E.-M. Aro, T. Müller, C. J. Howe and T. P. J. Knowles, *Nature Energy*, 2018, **3**, 75-81.
34. S. P. Mackay and P. J. O 'Malley, *Zeitschrift für Naturforschung C*, 1993, **48**, 191-198.
35. A. G. Roberts, M. K. Bowman and D. M. Kramer, *Biochemistry*, 2004, **43**, 7707-7716.
36. R. C. Honeycutt and D. W. Krogmann, *Plant Physiol*, 1972, **49**, 376-380.
37. K. Aizawa, *FEMS Microbiology Letters*, 1986, **39**, 215-233.
38. M. Wittmiß, S. Mikkat, M. Hagemann and H. Bauwe, *The Plant Journal*, 2020, **103**, 801-813.
39. E. M. Nichols, J. J. Gallagher, C. Liu, Y. Su, J. Resasco, Y. Yu, Y. Sun, P. Yang, M. C. Y. Chang and C. J. Chang, *Proc Natl Acad Sci U S A*, 2015, **112**, 11461-11466.
40. C. Liu, B. C. Colón, M. Ziesack, P. A. Silver and D. G. Nocera, *Science*, 2016, **352**, 1210-1213.
41. P. C. Sahoo, D. Pant, M. Kumar, S. K. Puri and S. S. V. Ramakumar, *Trends Biotechnol*, 2020, **38**, 1245-1261.
42. K. Rabaey and R. A. Rozendal, *Nature Reviews Microbiology*, 2010, **8**, 706-716.
43. K. P. Nevin, T. L. Woodard, A. E. Franks, Z. M. Summers and D. R. Lovley, *mBio*, 2010, **1**, e00103-00110.
44. X. Gao, F. Gao, D. Liu, H. Zhang, X. Nie and C. Yang, *Energy & Environmental Science*, 2016, **9**, 1400-1411.
45. M. Kanno, A. L. Carroll and S. Atsumi, *Nat Commun*, 2017, **8**, 14724.
46. M. R. Badger and G. D. Price, *J Exp Bot*, 2003, **54**, 609-622.
47. K. Schuchmann and V. Muller, *Nat Rev Microbiol*, 2014, **12**, 809-821.
48. M. C. Hanna and A. J. Nozik, *Journal of Applied Physics*, 2006, **100**, 074510.
49. C. H. Foyer, A. J. Bloom, G. Queval and G. Noctor, *Annual Review of Plant Biology*, 2009, **60**, 455-484.
50. X.-G. Zhu, S. P. Long and D. R. Ort, *Annual Review of Plant Biology*, 2010, **61**, 235-261.
51. W. Yamori and T. Shikanai, *Annual Review of Plant Biology*, 2016, **67**, 81-106.
52. J. G. K. Williams, in *Methods in Enzymology*, Academic Press, 1988, vol. 167, pp. 766-778.
53. A. Murakami, S. J. Kim and Y. Fujita, *Plant Cell Physiol*, 1997, **38**, 392-397.
54. A. Murakami and Y. Fujita, *Plant Cell Physiol*, 1993, **34**, 1175–1180.
55. C. Wu, H. Jiang, I. Kalra, X. Wang, M. Cano, P. Maness, J. Yu and W. Xiong, *Metab Eng*, 2020, **57**, 140-150.

56. P. C. Carvalho, D. B. Lima, F. V. Leprevost, M. D. Santos, J. S. Fischer, P. F. Aquino, J. J. Moresco, J. R. Yates and V. C. Barbosa, *Nat Protoc*, 2016, **11**, 102-117.
57. W. Xiong, L. Liu, C. Wu, C. Yang and Q. Wu, *Plant Physiol*, 2010, **154**, 1001-1011.
58. A. Nanchen, T. Fuhrer and U. Sauer, *Methods Mol Biol*, 2007, **358**, 177-197.
59. J. Ungerer, L. Tao, M. Davis, M. Ghirardi, P.-C. Maness and J. Yu, *Energy & Environmental Science*, 2012, **5**, 8998-9006.

Author contributions: W.X., J.B., D.S. project conception. Z.L., X.C., D.S., J.B., W.X. designed, performed, and/or analyzed photo-electrochemical experiments. Z.L., C.W., X.G., W.X. designed, performed, and/or analyzed biological experiments including cyanobacteria cultivation, spectroscopic analysis, metabolite analysis, ^{13}C-labeling and GC-MS. B.A. performed NMR analysis. S.S., X.W., C.W. performed proteomics analysis. W.X., J.B. wrote the manuscript with input from all authors and revisions from D.S. and J.Y.

Conflicts of interest: Authors declare no competing interests**.**

Acknowledgments

This work was authored in part by the National Renewable Energy Laboratory, operated by Alliance for Sustainable Energy, LLC, for the U.S. Department of Energy (DOE) under Contract No. DE-AC36-08GO28308. Funding for W.X., Z.L., and D.S., for cyanobacteria development, provided by the National Renewable Energy Laboratory Laboratory Directed Research and Development (LDRD) program. Funding for Z.L. and J.L.B., for photoelectrochemical design and experimentation, provided by the Solar Photochemistry Program, Division of Chemical Sciences, Geosciences, and Biosciences, Office of Basic Energy Sciences, U.S. Department of Energy (DOE). The views expressed in the article do not necessarily represent the views of the DOE or the U.S. Government. The U.S. Government retains and the publisher, by accepting the article for publication, acknowledges that the U.S. Government retains a nonexclusive, paid-up, irrevocable, worldwide license to publish or reproduce the published form of this work, or allow others to do so, for U.S. Government purposes. We acknowledge Dr. Wim Vermaas at Arizona State University for providing a Synechocystis PSII deficient mutant. We also thank Dr. Ji Hao for assistance on transport measurements.

680

681 **Figures and figure legends**

682

683 **Figure 1**

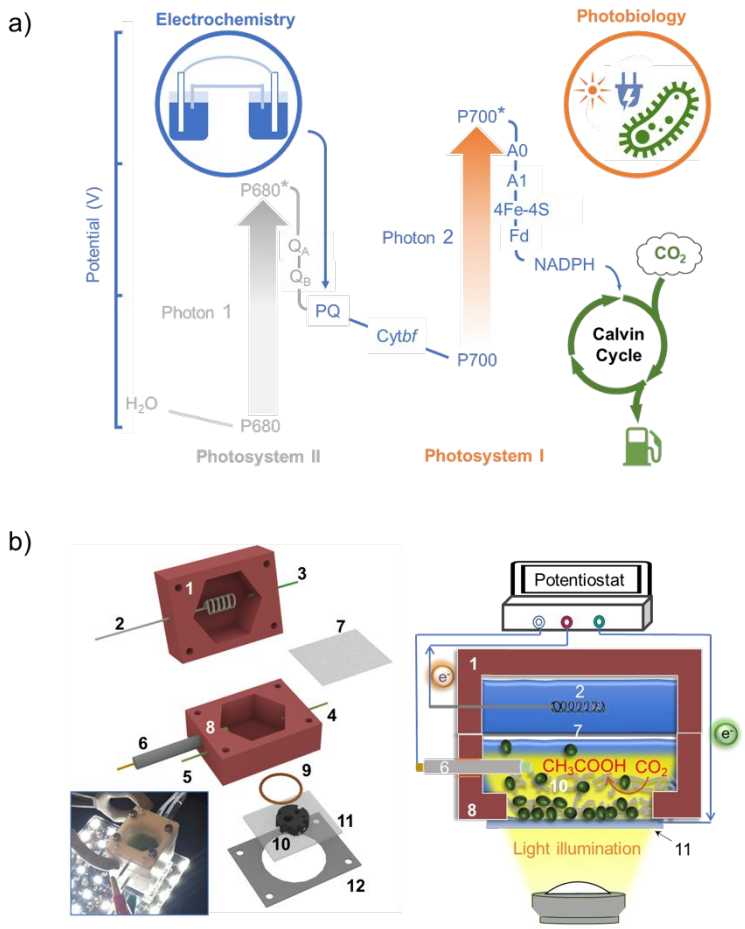

684

685 **Fig. 1. Electrophototrophic system**. **a)** The electrophototroph is designed for CO_2-to-
686 fuels conversion with external supply of light and electricity to a tailored photosynthetic
687 microbe. To this end, photosystem II in natural photosynthesis (gray) can be genetically
688 removed, and instead the external electrochemical circuit delivers high-energy electrons
689 to photoexcited photosystem I (oxidized P700), and ultimately produces NADPH to drive
690 CO_2 fixation. This process could leverage electron acceptors in the PETC including
691 plastoquinone (PQ), Cytochrome b6f complex (Cyt*bf*), special chlorophyll (A_0), vitamin K
692 (A_1), iron-sulfur centers (4Fe-4S), and ferredoxin (fd) *etc*. Protons can be pumped across
693 the thylakoid membrane establishing a proton-motive force that can be used for the
694 synthesis of ATP. **b)** Schematic illustration and photograph (inset of left panel) of

electrochemical device to shuttle electrons to PSII deficient cyanobacteria. Component 1 and 8: PTFE anodic part and cathodic part; Component 2: Platinum counter electrode; Component 3, 4, 5: medium inlet/outlet; Component 6: Ag/AgCl reference electrode; Component 7: Nafion Membrane; Component 9: Seal O-ring; Component 10: Carbon felt; Component 11: FTO glass; Component 12: Working electrode clamp. Right panel shows the loading of cyanobacterial cells and the electrons delivery process.

Figure 2

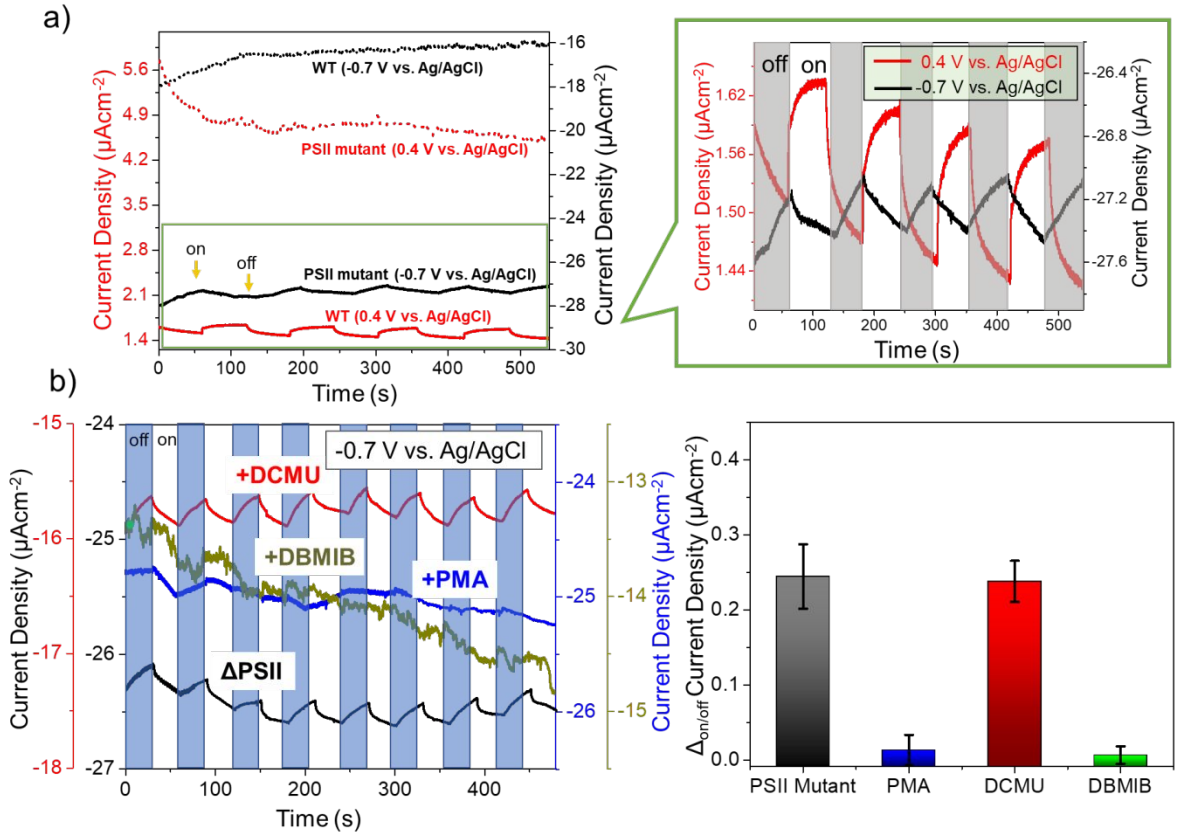

Fig. 2. Electrochemical properties of the electrophototrophic hybrid. **a)** i-t measurement under chopped illumination when cyanobacterial cells (*Synechocystis* WT and ΔPSII mutant) were applied as electron donor (on anode, red solid and dash line) or acceptor (on cathode, black solid and dash line). Right panel comparing the light-response of WT and ΔPSII cells as electron donor and acceptor, respectively. **b)** Current density changes in response to light/dark switch with addition of site-specific PETC inhibitors individually to cathodic ΔPSII culture. The time-course and differences of current density between light and dark are shown on the left and right panel, respectively. Left plot shows a representative result from biological replicates (n=3). Error bars in the right panel represent standard deviations for replicates of photocurrent density (differences between light on and off (n=5)). See Fig. S12 for a negative control, in which the current density changes are in response to light/dark switch with addition of all site-specific PETC inhibitors (DCMU, DBMIB and PMA).

717

718

719 **Figure 3**

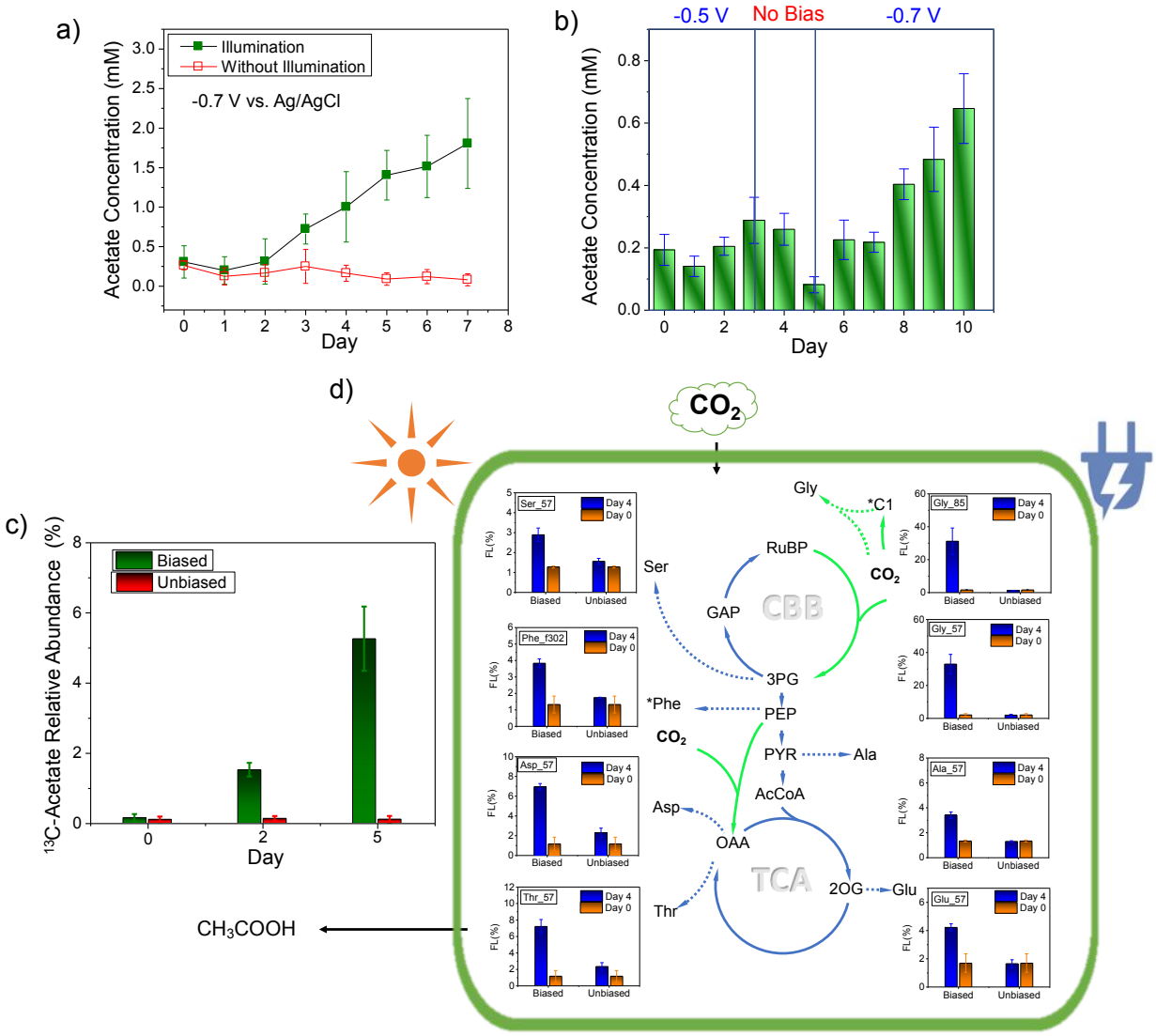

720

721 **Fig. 3. CO_2 valorization by the electrophototrophic hybrid**. **a)** Electrophototrophic
722 acetate production of ΔPSII by external electrical bias (-0.7 V vs. Ag/AgCl) with and
723 without illumination. **b)** Time course of electrophototrophic productivity for ΔPSII under
724 illumination with different electron supplies. Error bars represent standard deviations from
725 biological triplicates. **c)** ^{13}C-acetate production via fixation of $^{13}CO_2$ (derived from ^{13}C-
726 bicarbonate) in illuminated ΔPSII, with or without application of external electrical bias (-

727 0.7 V vs. Ag/AgCl). **d)** Fractional labeling of seven protein-bound amino acids that were
728 directly produced from the central carbon metabolism via fixation of $^{13}CO_2$ (derived from
729 ^{13}C-bicarbonate) in illuminated ΔPSII, with or without application of external electrical bias
730 (-0.7 V vs. Ag/AgCl). Green arrows indicate CO_2-fixing reactions. Dash lines are reactions
731 for the synthesis of amino acids. Abbreviations: RuBP, ribulose 1,5-bisphosphate; GAP,
732 glyceraldehyde 3-phosphate; 3PG, 3-phosphoglycerate; PEP, phosphoenolpyruvate;
733 PYR, pyruvate; AcCoA, acetyl coenzyme A; OAA, oxaloacetate; 2OG, 2-oxoglutarate.
734 CBB, the Calvin-Benson-Bassham Cycle; TCA, the tricarboxylic acid cycle. Amino acids
735 are presented by their 3-letter abbreviations. *Phe indicates partial carbons of
736 phenylalanine (C1-3) synthesized from PEP. *C1 indicates that one carbon unit is the
737 precursor of glycine's methylene group and can be represented by the Gly_85 fragment
738 in GC-MS. All electricity and illumination supply were programed as "30 s supply + 30 min
739 interval".

740 **Figure 4**

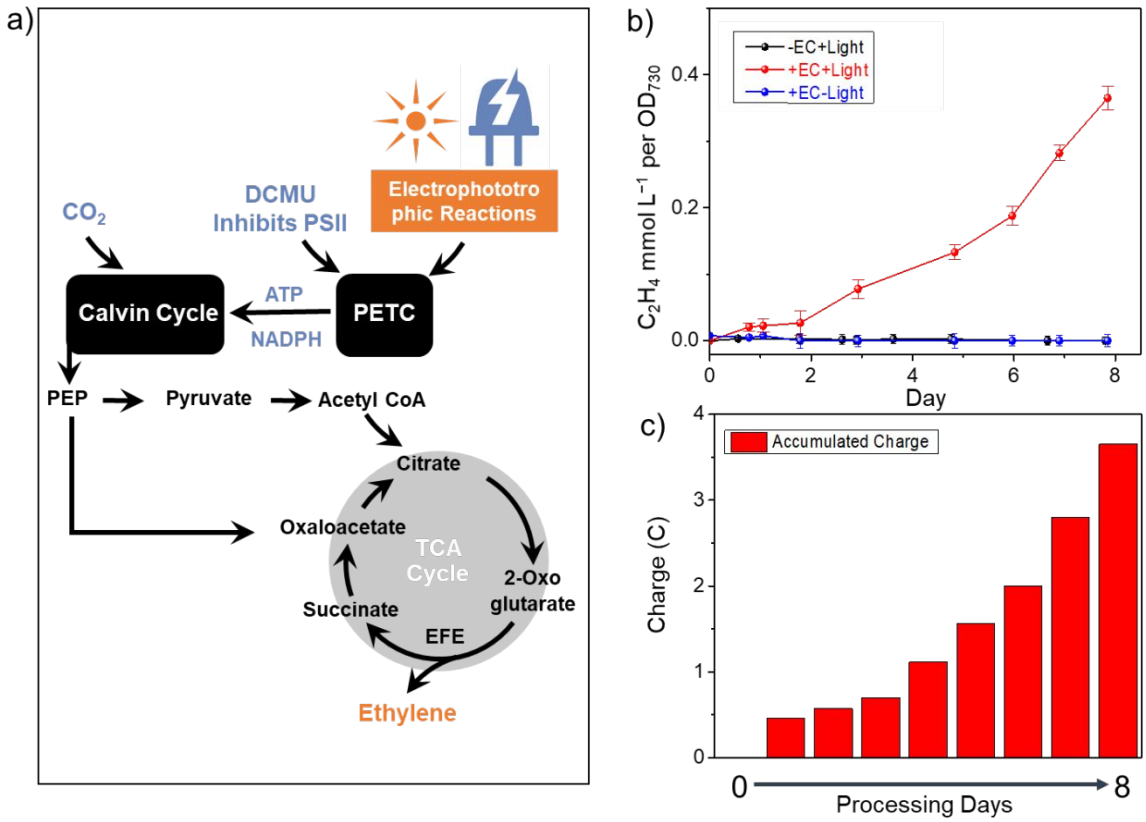

741
742 **Fig. 4. Electrophototrophic ethylene production in cyanobacteria. a)** The pathway
743 for electrophototrophic ethylene production in engineered *Synechocystis* JU547[8].
744 Electrophototrophic reactions are triggered by exogenous electricity supply, light
745 illumination, and inhibition of PSII with DCMU. The conversion of CO_2 into ethylene is
746 then energized by ATP and NADPH and enabled through an heterologously expressed
747 ethylene forming enzyme (EFE). **b)** Successive ethylene production from
748 electrophototrophic cyanobacteria in the presence (+) or absence (-) of electric bias (EC,
749 -0.7V vs. Ag/AgCl) and light (55 μmol m^{-2} s^{-1}). Error bars represent biological triplicates.
750 **c)** Total charges, in Coulombs, that were accumulatively applied to the cathodic culture
751 for ethylene production. All electricity and illumination supply were programed as "30 s
752 supply + 30 min interval".

754